



HAL
open science

Supramolecular Self-Organization of Potential Hydrogelators on Attracting Surfaces

Arno M. Bieser, Joerg C. Tiller

► **To cite this version:**

Arno M. Bieser, Joerg C. Tiller. Supramolecular Self-Organization of Potential Hydrogelators on Attracting Surfaces. *Supramolecular Chemistry*, 2009, 20 (04), pp.363-367. 10.1080/10610270701260325 . hal-00513506

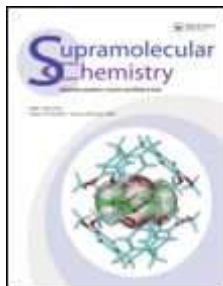
HAL Id: hal-00513506

<https://hal.science/hal-00513506>

Submitted on 1 Sep 2010

HAL is a multi-disciplinary open access archive for the deposit and dissemination of scientific research documents, whether they are published or not. The documents may come from teaching and research institutions in France or abroad, or from public or private research centers.

L'archive ouverte pluridisciplinaire **HAL**, est destinée au dépôt et à la diffusion de documents scientifiques de niveau recherche, publiés ou non, émanant des établissements d'enseignement et de recherche français ou étrangers, des laboratoires publics ou privés.



Supramolecular Self-Organization of Potential Hydrogelators on Attracting Surfaces

Journal:	<i>Supramolecular Chemistry</i>
Manuscript ID:	GSCH-2006-0126.R1
Manuscript Type:	Full Paper
Date Submitted by the Author:	02-Feb-2007
Complete List of Authors:	Bieser, Arno; University of Freiburg Tiller, Joerg; University of Freiburg
Keywords:	Supramolecular, Self-Assembly, Low Molecular Weight, Hydrogelator
<p>Note: The following files were submitted by the author for peer review, but cannot be converted to PDF. You must view these files (e.g. movies) online.</p> <p>Figure 1.cdx</p>	



Supramolecular Self-Organization of Potential Hydrogelators on Attracting Surfaces

Arno M. Bieser and Joerg C. Tiller*

*Freiburg Materials Research Center and Institute for Macromolecular Chemistry, Stefan-Meier-Str.21, 79104 Freiburg, Germany. Tel: +49(0)761 203-4735; Fax: +49(0)761 203-4709; E-mail: joerg.tiller@mf.uni-freiburg.de

Abstract

This article highlights the aggregation behaviour of potential low molecular weight hydrogelators on **attracting surfaces**. Our goal was the development of a method, which enables the finding of new hydrogelators that are not easily recognizable as such because they only form instable or no hydrogels in aqueous solution. To this end, a series of negatively charges azo-dyes was synthesized and positive charged glass slides were immersed into their aqueous solutions. All dyes showed supramolecular organization and significant concentration on the attracting glass surface. Microscopic investigations mostly revealed the formation of crystals. However, one compound, **(1-(2-n-Octylphenylazo)-2-hydroxy-6-naphthalenesulphonate)**, selectively formed a hydrogel on the surface whereas it does not gel in aqueous solution. This reveals the hydrogel as **the stable form of this compound** under equilibrium conditions. This method of surface-induced hydrogelation might facilitate the identification of new hydrogelators. Furthermore, it might also allow the mimicking of surface gelation as a process of biological relevance.

Keywords: Supramolecular, Self-Assembly, Low Molecular Weight, Hydrogelator.

INTRODUCTION

Self organization of molecules in water has drawn much attention and is an important topic for understanding and mimicking many processes in living organisms. In this context low molecular weight hydrogelators (LMWH) are the least understood class of molecules. Although such compounds have been found to be capable of gelling water more than hundred years ago [1] not many LMWH are known to date. Recent overviews and examples of these are presented in the reviews of Hamilton [2] and van Esch [3]. Amongst those, a hand full is known to form a hydrogel by dissolving the compound in water upon heating and subsequent

1
2
3 cooling to room temperature. The majority of the described hydrogelators require additives.
4 Such was already the case with the first hydrogelators found by Lipowitz in the course of his
5 experiments about the solubility of uric acid. To obtain gels, he needed to add certain bases
6 and salts like borax. Absence of these additions led to precipitation only. Equally is the
7 finding with many other hydrogelators described in literature. In some cases, the addition of
8 buffers like sodium carbonate [4,5] and others [6] is required. Jørgensen et al. report about
9 hydrogelators which necessitate adding of ethanol or dimethylformamide [7]. Also mixtures
10 with methanol [8] and other alcohols [9] or DMSO [10,11] etc. are common. Some gels are
11 only formed during their chemical synthesis or the subsequent workup procedure [12,13,14].
12 This is due to the fact that all hydrogelators must reach the minimal gelling concentration
13 (MGC) at a certain temperature and precipitate in form of a gel.

14
15
16
17
18
19
20
21
22
23 **The basis for gelation of LMWHs** are physical interactions like hydrophobic associations and
24 Van der Waals forces [15], hydrogen bonding [11,16], ionic bonding [17] and combination of
25 these forces [18]. **Another important factor for hydrogelling is the delicate**
26 **hydrophilic/hydrophobic balance of the compounds.** In an initial stage, the ordering of single
27 molecules leads to a primary structure which then can associate to build a secondary structure
28 of nano- to micrometer dimension, often with morphologies like fibres [18], micelles [15] or
29 ribbons [19]. Finally, interconnection of these leads to a tertiary structure that entraps the
30 water and forms a hydrogel. Since the bonds between the molecules are all non-covalent, each
31 of these association steps is reversible. Therefore, hydrogels of LMWH represent unique and
32 delicate systems where the right balance between order and disorder has to be found. Thus,
33 most likely a tremendous number of possibly hydrogel forming compounds exists and cannot
34 be recognized as such, because the molecules do not reach their MGC in water. Until now
35 there is no established procedure that can mimic the gelation behaviour of a hydrogelator
36 below MGC. Here, we describe a method that reveals the hydrogel forming potential of low
37 molecular weight compounds that do not reach MGC in their aqueous solutions.
38
39
40
41
42
43
44
45
46
47
48
49
50

51 **RESULTS AND DISCUSSION**

52 **Organization properties during synthesis**

53 Hamada et al. examined the gelling properties of diverse azo-dyes composed of 2-naphthol-6-
54 sulphonic acid and different anilines which form instable hydrogels [20,21]. Based on these
55 findings, we synthesized a library of various regioisomers containing diverse side chains at
56 the ortho-, meta- and para-position to the azo-group (Table 1 and Fig. 1). As described
57 previously, it was found that only one of the isolated azo dyes (1-(2-n-Hexylphenylazo)-2-
58
59
60

1
2
3 hydroxy-6-naphthalenesulphonate (**5-o**) forms a stable and thermoreversible hydrogel and is
4 also capable of gelling on appropriately modified **attracting** surfaces [22]. However, many of
5 the other compounds did form hydrogels during their synthesis but these gels form
6 precipitates with time (Table 1 and Fig. 2).
7
8
9

10 *Figure 1*

11 *Table 1*

12 *Figure 2*

13
14
15
16
17
18 The formation of precipitates was temperature dependent. While the hydrogels were stable at
19 5 °C for several hours, they precipitated within minutes when warmed to room temperature.
20 This finding seems to indicate that the hydrogels are not thermodynamically stable and the
21 reorganization is kinetically controlled. We presume that the gelation occurred during
22 synthesis, where the highly concentrated educts form the respective azo dye during a fairly
23 fast reaction. Thus, the product exceeds its solubility product and also its MGC very fast. If
24 the compound has hydrogelling abilities, it will form a gel in the first place, because this is the
25 fastest way to remove its hydrophobic moieties out of the water. However, if this gel is not the
26 stable form under the conditions at hand, the compound then crystallizes with time. In the
27 cases of compounds **6-o**, **6-p**, and **7-p**, it is thinkable that the solubility product is exceeded,
28 but not MGC, which then results in the formation of an amorphous precipitate.
29

30
31
32
33
34
35
36
37
38
39
40
41
42
43
44
45
46
47
48
49
50
51
52
53
54
55
56
57
58
59
60
In all later attempts, it was not possible to obtain again gels from the precipitates by heating
the reaction mixtures and subsequent cooling. Obviously, MGC of these compounds cannot
be reached anew this way. This phenomenon was already described for other hydrogels as
well [23].

Organization properties on attracting surfaces

To explore the self-organization properties of the isolated azo dyes, they were saturated in
boiling water and the solution was cooled to room temperature. In all cases with the exception
of **5-o** precipitation of crystals or amorphous substances but no hydrogelation occurred, **i.e.**
the MGC was not reached. However, all aqueous solutions with concentrations below 1 wt.%
did not show precipitates.

In order to obtain a **stable** self-organization form **of the pure azo dyes from the aqueous
solution in concentrations above MGC**, we decided to explore the interactions of stable dye
solutions with NH₂ functionalized surfaces. Since the negatively charged dyes show an
electrostatic affinity to amino groups, they will have a higher concentration near the surface as

1
2
3 known from many other examples [24,25,26,27]. In the ideal case, this surface concentration
4 exceeds the concentration required for the compounds to form supramolecular structures,
5 which will then be formed on the surface only. The amino glass slides have been immersed
6 into solutions with concentrations of 0.4 wt.%. After 16 h, the slides were removed and
7 examined under a light microscope. Whereas none of the dyes precipitated from their
8 solutions under normal conditions or on unmodified glass slides, we always found depositions
9 of the dyes on the amino glass slides. Investigations of the latter revealed 4 scenarios: cubic
10 crystals (Fig. 3b), sheet-like crystals (Fig. 3c), amorphous aggregates mixed with crystals, and
11 very surprisingly a highly ordered non-crystalline structure in the case of **7-o** (Fig. 3d). Table
12 2 summarizes the results of these experiments.
13
14
15
16
17
18
19
20
21
22

23 *Table 2*

24
25
26 As seen in Fig. 3a, dense coatings of fairly regular crystals had been formed in many cases.
27 The dimensions of the crystals ranged from 10 to 50 μm as for **4-o** but also up to some
28 hundred micrometers as for the **4-p**. This crystallization is noteworthy since azo dyes usually
29 do not exhibit good crystallizing properties [28].
30
31
32
33
34

35 *Figure 3*

36
37
38 To get a closer look at the morphologies of the aggregates, the samples were freeze dried and
39 examined with an environmental scanning electron microscope (ESEM). It turned out, that the
40 crystals possess sandwich structures with stacked layers (Fig. 4 a-d). In the cubic crystals,
41 these layers are dense-packed with little to no gap visible (Fig. 4b and 4d) whereas the layers
42 of the sheet like crystals seem to be stapled more loosely on top of each other (Fig. 4a and
43 4c). Mostly, the layers in the sheet like systems are of the same shape and dimension with
44 very accurate superimposition. Therefore, the crystals are quite regular. The cubic crystals are
45 less regular since the individual layers are often of different dimensions. Finally, it is worth
46 noting that the sheet like morphology was only observed for the para-substituted azo dyes
47 whereas the ortho-analogues frequently exhibited the cubic shape . This shows that the
48 position of the alkyl-group has an important influence on the crystallizing behaviour of the
49 dyes.
50
51
52
53
54
55
56
57
58
59
60

1
2
3
4
5
6
7
8
9
10
11
12
13
14
15
16
17
18
19
20
21
22
23
24
25
26
27
28
29
30
31
32
33
34
35
36
37
38
39
40
41
42
43
44
45
46
47
48
49
50
51
52
53
54
55
56
57
58
59
60

Figure 4

Figure 5

As seen in Fig. 5a, the ESEM image of the structure of freeze-dried samples of **7-o** is very regular in a honey-comb like fashion. The structure does not resemble crystals but exactly the structure of the xerogel of surface-induced hydrogels of hydrogelator **5-o** (Fig. 5b) of our previous experiments [22]. Thus, **7-o** obviously formed a hydrogel on the surface of the amino glass slide. In contrast to all the other investigated dyes, the hydrogel seems to be the stable form of **7-o**. This is surprising, because during synthesis, **7-o** formed only an instable hydrogel, which precipitated rather quickly. This might be explained by the fact that the concentration of **7-o** then was too high or the salts or other impurities in the reaction mixture induced precipitation.

CONCLUSION

In closing, hydrogelation is undoubtedly a phenomenon that is still poorly understood and much research has to be done in order to broaden the understanding in this field. Here, it could be demonstrated for the first time, that surface-induced self-organization seems to be a useful tool to get closer insights in the potential of low molecular weight compounds to form hydrogels. This simple yet informative experiment might serve as new procedure to find out **the stable form of a compound under equilibrium conditions** and thus might be a new method for the identification of potential hydrogelators which have been overseen as such previously. Furthermore, since it can be done under any chosen conditions including the application of tailored surfaces with specific recognition structures, surface-induced hydrogelation might enable the investigation of hydrogelling drugs, e.g. the pyrene-modified vancomycin, under physiological conditions [29,30].

EXPERIMENTAL

Azo coupling: A typical method is described on the example of **7-o**. The diazonium salt of 2-octyl-aniline was prepared by slow addition of a solution of sodium nitrite (2.42 g, 35 mmol) in water (5 ml) to a solution of the aniline (6.20 g, 35 mmol) in water (15 ml) and conc. hydrochloric acid (7.8 ml, 95 mmol) at 5 °C. This solution was slowly added to a solution of 2-naphtholsulfonic acid sodium salt (8.64 g, 35 mmol) and sodium hydroxide (4.00 g, 100 mmol) in water (100 ml) at 5 °C. After addition of the first 5 ml of diazonium salt solution, the mixture became viscous and started to form a hydrogel. To isolate the product after

complete reaction, sodium chloride (35 g) was added and the product was precipitated at 5 °C over night. The residue was recrystallized repeatedly from a mixture of ethanol/methanol/acetone/water (3:3:4:1, v:v:v:v).

Surface-induced aggregation: Solutions of azo dyes have been prepared by dissolving the 0.4 wt.% of dyes in distilled and boiling water. After cooling to room temperature, amino glass slides have been placed into these solutions for 16 h. Finally, the slides were removed and investigated under the microscope in wet condition or the ESEM after freeze drying.

Visible microscopy images were measured with an Axioplan 2 imaging microscope (Zeiss, Jena, Germany). **Scanning electron microscope images** were recorded with an ESEM 2020 (Electron Scan Corporation, Wilmington, MA, USA) after previous sputtering with gold palladium in a Polaron Sputter Coater SC 7640.

Supporting Information Available

Analytical data for all azo dyes as well as the preparation procedure for the amino glasses and further azo-coupling experiments are available.

Acknowledgements

This work was supported by the Deutsche Forschungsgemeinschaft (Emmy-Noether-Programm) and by the Fonds der Chemischen Industrie. The authors thank Rainer Wissert and Dr. Andreas Pfister for the ESEM measurements.

References

- [1] Lipowitz A. *Ann. Chem. Pharm.* **1841**, 38, 348.
- [2] Estroff L.; Hamilton A.D. *Chem. Rev.* **2004**, 104, 1201.
- [3] De Loos, M.; Feringa, B.L.; van Esch, J.H. *Eur. J. Org. Chem.* **2005**, 3615.
- [4] Yang, Z.; Gu, H.; Zhang, Y.; Wanga, L.; Xu, B. *Chem. Commun.* **2004**, 208.
- [5] Sreenivasachary, N.; Lehn, J.-M. *Proc. Natl. Acad. Sci.* **2005**, 102, 5938.
- [6] Newkome, G.R.; Baker, G.R.; Arai, S.; Saunders, M.J.; Russo, P.S.; Theriot, K.J.; Moorefield, C.N.; Rogers, L.E.; Miller, J.E.; Lieux, T.R.; Murray, M.E.; Phillips, B.; Pascal, L. *J. Am. Chem. Soc.* **1990**, 112, 8458.
- [7] Jørgensen, M.; Bechgaard, K.; Bjørnholm, T.; Sommer-Larsen, P.; Hansen, L.G.; Schaumburg, K. *J. Org. Chem.* **1994**, 59, 5877.
- [8] Jung, J.H.; John, G.; Masuda, M.; Yoshida, K.; Shinkai, S.; Shimizu, T. *Langmuir* **2001**, 17, 7229.
- [9] Gradzielski M.; Müller, M.; Bergmeier, M.; Hoffmann, H.; Hoinkis, E. *J Phys Chem B* **1999**, 103, 1416.
- [10] Hirst, A.R.; Smith, D.K. *Top. Curr. Chem.* **2005**, 256, 237.
- [11] Menger, F.M.; Caran, K.L. *J. Am. Chem. Soc.* **2000**, 122, 11659.
- [12] Snijder, C.S.; De Jong, J.C.; Meetsma, A.; Van Bolhuis, F.; Geringa, B.L. *Chem. Eur. J.* **1995**, 1, 594.
- [13] Iwanowicz, E.I.; Poss, M.A.; Lin, J. *Synth. Commun.* **1993**, 10, 1443.
- [14] Menger, F.M.; Yamasaki, Y.; Catlin, K.K.; Nishimi, T. *Angew. Chem. Int. Ed. Engl.* **1995**, 34, 585.
- [15] Fuhrhop, J.-H.; Boettcher, C. *J. Am. Chem. Soc.* **1990**, 112, 1768.
- [16] Das, D.; Dasgupta, A.; Roy, S.; Mitra, R.N.; Debnath, S.; Das, P.K. *Chem. Eur. J.* **2006**, 12, 5068.
- [17] Nakashima, T.; Kimizuka, N. *Adv. Mater.* **2002**, 14, 1113.
- [18] John, G.; Masuda, M.; Okada, Y.; Yase, K.; Shimizu, T. *Adv. Mater.* **2001**, 13, 715.
- [19] Boettcher, C.; Schade, B.; Fuhrhop, J. H. *Langmuir* **2001**, 17, 873.

- 1
2
3 [20] Hamada, K.; Yamada, K.; Mitsuishi, M.; Ohira, M.; Miyazaki, K. *J. Chem. Soc. Chem. Commun.* **1992**,
4 544.
5 [21] Hamada, K.; Take, S.; Iijima, T.; Amiya, S. *J. Chem. Soc., Faraday Trans. 1* **1986**, 82, 3141.
6 [22] Bieser, A.M.; Tiller, J.C. *Chem. Commun.* **2005**, 31, 3942.
7 [23] Haller, R. *Kolloid Z.* **1918**, 22, 49.
8 [24] Karukstis, K.K.; Perelman, L.A.; Wong, W.K. *Langmuir* **2002**, 18, 10363.
9 [25] Horobin, R.W.; Bennion, P.J. *Histochem. and Cell Biol.* **1972**, 33, 191.
10 [26] Armagan, B.; Ozdemir, O.; Turan, M.; Çelik, M.S. *J. Envir. Engrg.* **2003**, 129, 709.
11 [27] Ray, K.; Nakahara, H. *Bull. Chem.Soc. Jap.* **2002**, 7, 1493.
12 [28] Chisholm, G.; Kennedy, A.R.; Wilson, S.; Teat, S.J. *Acta Cryst.* **2000**, B56, 1046.
13 [29] Xing, B., Yu, C.-W., Chow, K.-H., Ho, P.-L., Fu, D., Xu, B. *J. Am. Chem. Soc.* **2002**, 124, 14846.
14 [30] Tiller, J.C. *Angew. Chem.* **2003**, 42, 3072.
15
16
17
18

19 Tables

20
21
22 TABLE 1 Synthesized azo-dyes and their behaviour during synthesis: G: instable hydrogel
23 formed during synthesis, GG: stable hydrogel formed from the aqueous solution, D: no
24 hydrogel and no precipitate during synthesis, P: precipitation during synthesis.
25
26
27

	R	<i>o</i> -	<i>m</i> -	<i>p</i> -	
28					
29	1	CF ₃	G	G	-
30	2	C ₂ H ₅	G	D	-
31	3	n-C ₄ H ₉	G	G	G
32	4	n-C ₅ H ₁₁	G	-	G
33	5	n-C ₆ H ₁₃	GG	G	G
34	6	n-C ₇ H ₁₅	P	-	P
35	7	n-C ₈ H ₁₇	G	-	P

36
37
38
39
40
41
42
43
44
45
46
47 TABLE 2 Type of deposition of the azo-dyes on amino glass surface: C: crystallization – CC:
48 cubic crystals, SC: sheet like crystals, G: Gelation, C&A: formation of crystals and
49 amorphous aggregates.
50
51
52
53

#	R	<i>o</i> -	<i>m</i> -	<i>p</i> -	
54	1	CF ₃	C	C	-
55	2	C ₂ H ₅	C&A	C&A	-
56	3	n-C ₄ H ₉	CC	CC&A	C
57	4	n-C ₅ H ₁₁	CC	-	SC

5	n-C ₆ H ₁₃	G	SC&A	SC
6	n-C ₇ H ₁₅	CC	-	C&A
7	n-C ₈ H ₁₇	G	-	C

Figures

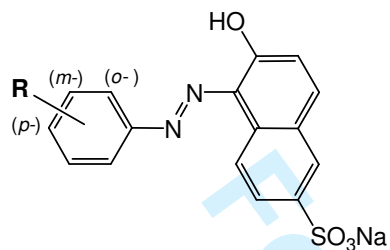


FIGURE 1 Chemical Motive of the synthesized Azo-Dyes

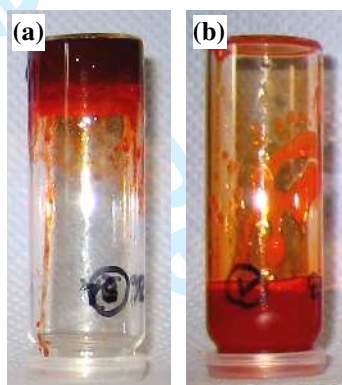


FIGURE 2 (a) Hydrogel of **5-p** with 4,7 wt.-% formed during synthesis at 5 °C, (b) precipitated sample after warmed to room temperature.

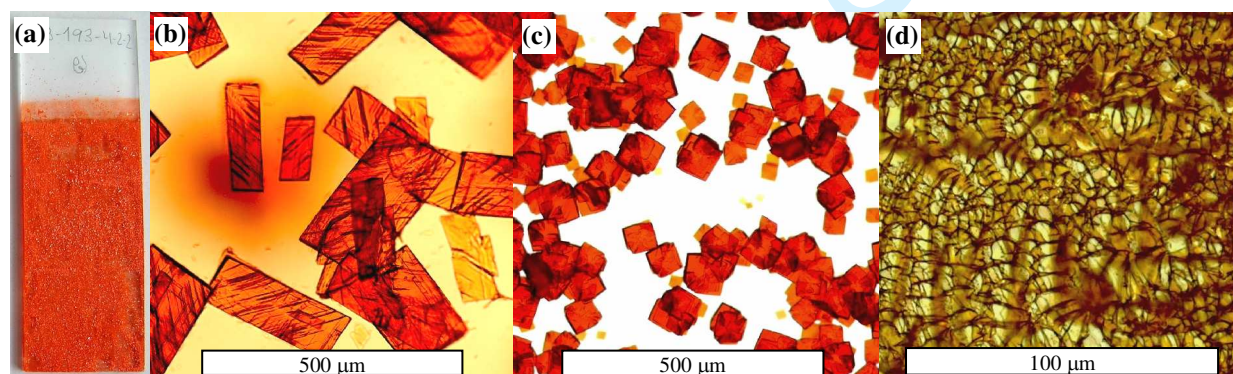
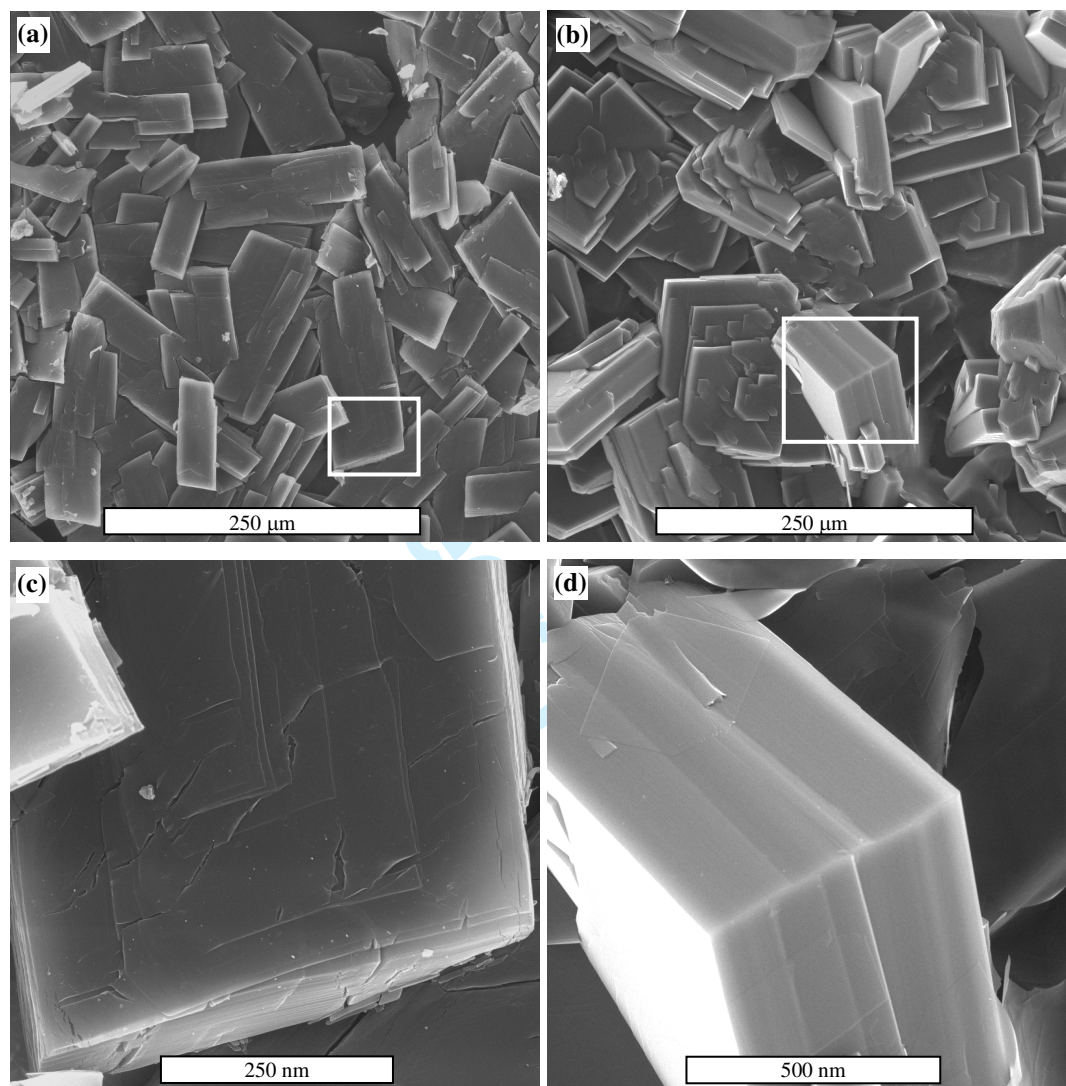


FIGURE 3 (a) Amino glass surface showing deposition of crystals of **4-p** formed from a solution of 0.4 wt.-%, (b) light microscopy image of such crystals, (c) light microscopy image

1
2
3 of crystals of the **4-o** from a solution of 0.4 wt.-%, (d) Light microscopy image of a amino
4 glass surface after immersion into a 0,4 wt.-% solution of **o-7** showing the regular structuring.
5
6
7
8



45
46 FIGURE 4 SEM images of surface grown crystals of (a) **4-p**, (b) **3-o**. (c) and (d) show
47 magnifications of the highlighted areas of the pictures above.
48
49
50
51
52
53
54
55
56
57
58
59
60

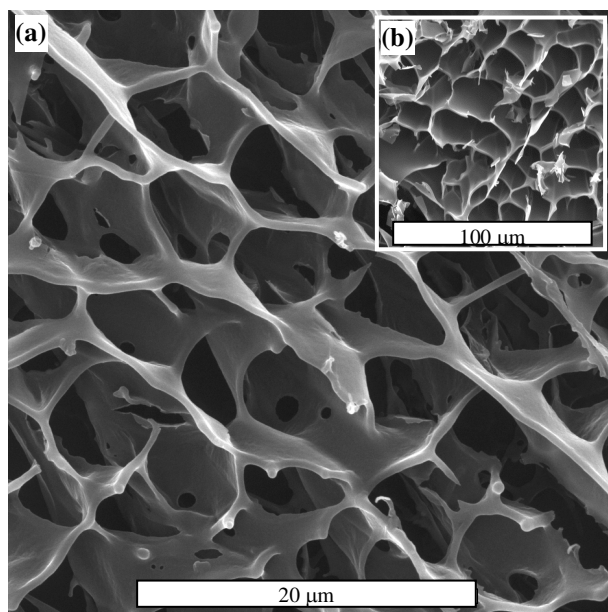


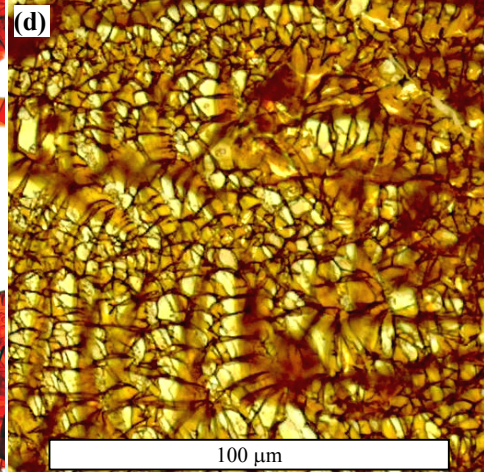
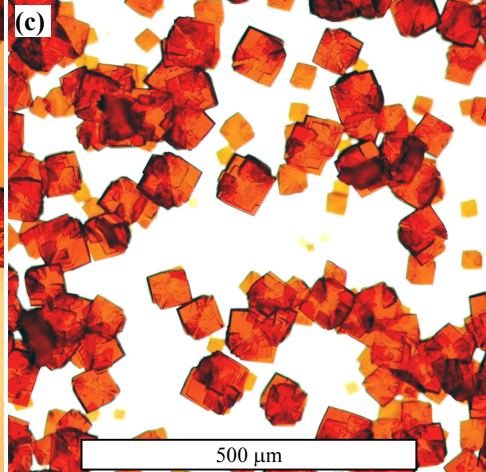
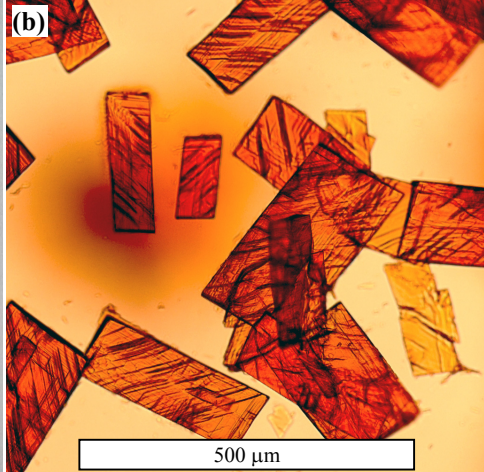
FIGURE 5 SEM images of (a) the surface induced structuring of **7-o**, (b) of a xerogel sample of a surface-grown hydrogel of **5-o**.

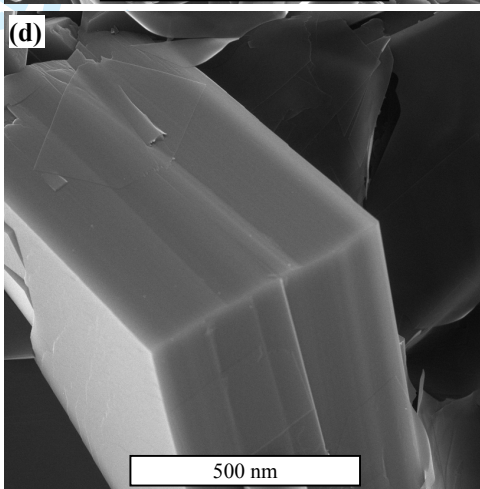
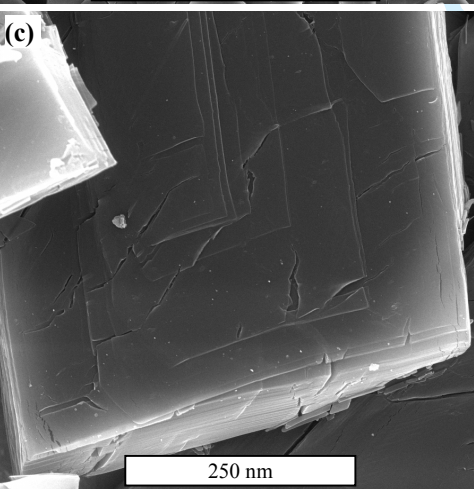
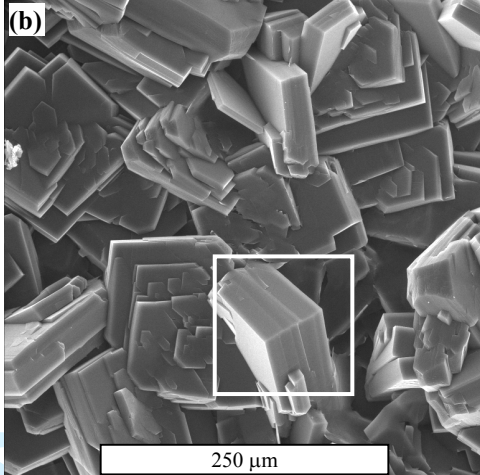
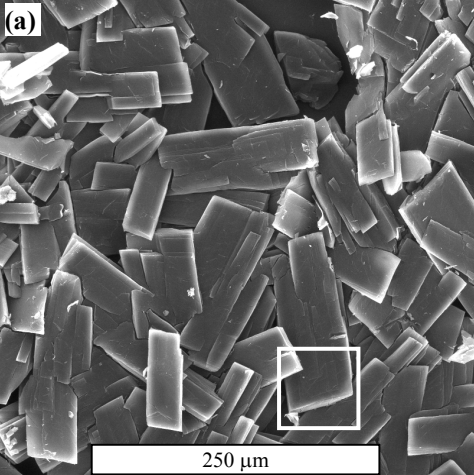
(a)

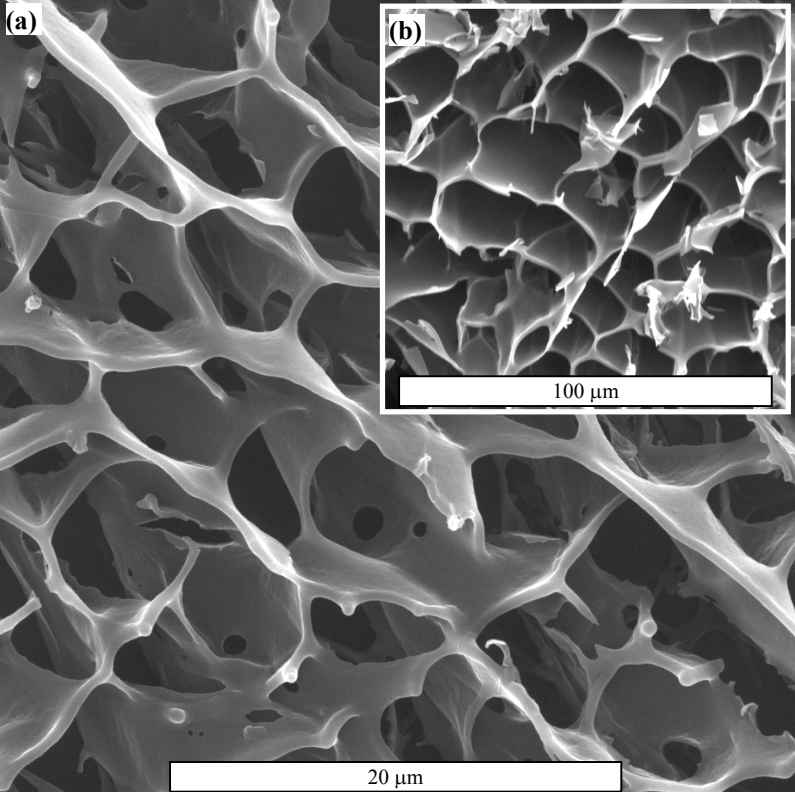


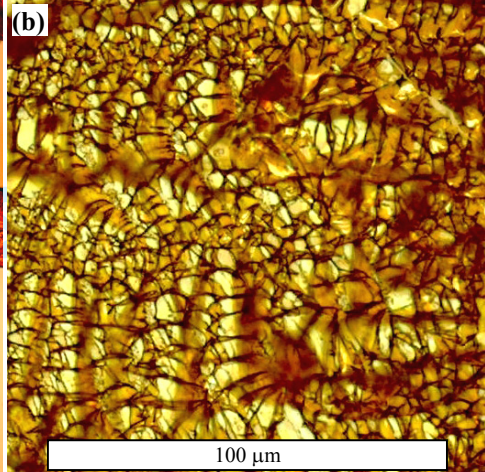
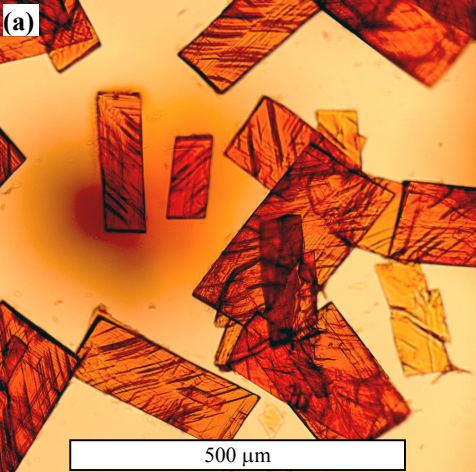
(b)











SUPPORTING INFORMATION

Supramolecular Self-Organization of Potential Hydrogelators on Attracting Surfaces

Arno M. Bieser and Joerg C. Tiller*

MATERIALS AND METHODS:

A) Unless otherwise noted, NMR spectra were recorded at room temperature in CDCl₃ or Dimethyl sulfoxide-d₆ in a Bruker ARX 300 spectrometer operating at respectively 300 and 75.4 MHz. Chemical shifts are reported relative to residual non-deuterated solvent.

B) Infrared spectra were obtained as films and as pellets (KBr) on a Bruker Vector 22 spectrometer.

C) Elemental analysis was done in the Institute of Organic Chemistry of the University Freiburg on a Elementar Vario EL.

D) Visible Microscopy images were taken with an Axioplan 2 imaging microscope (Zeiss, Jena, Germany).

E) Scanning electron microscope images were measured with an ESEM 2020 (Electron Scan Corporation, Wilmington, MA, USA) after previous sputtering with gold palladium in a Polaron Sputter Coater SC 7640.

F) Chemical reagents were used as received from commercial sources. The anilines for the synthesis of the Trifluoromethyl-substituted azo-dyes as well as the anilines for the ethyl-substituted azo-dyes have been obtained from Sigma-Aldrich and used without further purification. The other anilines have been synthesized according to literature procedures. No attempt was made to optimise yields. All solvents were purified and dried according to standard procedures.¹ Silica gel (60-200 mesh) for column chromatography was obtained from ICN-Biomedicals and Macherey-Nagel. Thin layer chromatography (TLC) was performed on Merck silica gel 60 F₂₅₄ (aluminium foil).

GENERAL PROCEDURES:

G) Amino glasses:

Amino glass slides were prepared by heating standard microscope glass slides in a solution of dry toluene (56 ml) and 3-Aminopropyl-trietoxysilane (14 ml) at 65 °C for 3 h. The slides were then carefully rinsed with water and dried over night at 70 °C.

I) "Hydrogelling" Azo coupling:

A volumetric standard solution of 2-naphtholsulfonic acid sodium salt in water with 250 mmol/l has been prepared. To this solution, 2 equivalents of sodium hydroxide have been added and the mixture was cooled to 5 °C (in the following conferred as sol. 1). Next, 12.5 mmol of the aniline together with 2.5 equivalent of 5 N hydrochloric acid have been dissolved in 30 ml distilled water in a volumetric flask of 50 ml volume. To this

¹ *Purification of Laboratory Chemicals*, EDs.: D. D. Perrin, W. L. F., Armarego, Pergamon Press, Oxford 1980.

solution, 1 equivalent of sodium nitrite as 2.5 N solution in water was slowly added at 5 °C under vigorous stirring. After 20 min., the volumetric flask was filled exactly to 50 ml by addition of water giving a volumetric standard solution of diazonium salt with 250 mmol/l (in the following conferred as sol. 2). The azo coupling reactions have been done in 10 ml sample flasks. The flask was put into an ice bath and equipped with magnetic stirring. Each reaction was done with the same volumes of reactant solutions. To obtain different concentrations of dye in the various reactions, an appropriate volume of pure water was put in the flask before addition of the reactant solutions. Then, the measured volumes of the reactants have been added simultaneously via pipette. The total volume of each reaction was adjusted between 2 and 6 ml by taking the appropriate amounts of water and reactant solutions. Gelation was considered to have occurred when a homogeneous substance was obtained that exhibited no gravitational flow when turning the vial upside down. The following table (Table 1) gives the experimental data for coupling reactions of the azo-dye **5-p**. Other experiments with other dyes have been performed in a similar manner, sometimes however with different concentrations or volumes. Table 2 provides an overview about the findings in the various experiments.

Table 1 Experimental Data for the Azo Coupling of 5-p.^a

#	V(H ₂ O) [μl]	V(sol. 1) [μl]	V(sol. 2) [μl]	max. conc. [mmol/l]	max. wt.-%	observation
1	4000	500	500	25.00	1.09	d
2	3500	1000	1000	45.45	1.98	d
3	1600	1000	1000	69.44	3.02	d
4	1000	1500	1500	93.75	4.07	s
5	500	1500	1500	107.14	4.66	s
6	0	1000	1000	125.00	5.43	p

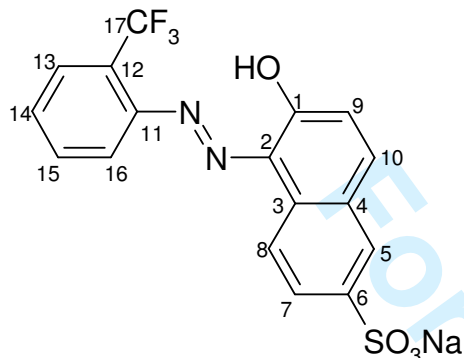
^as: stable gel during synthesis, d: dissolved, p: precipitation.

Table 2 Azo-Dyes and their Behaviour during Synthesis^a

R	<i>o</i> -	<i>m</i> -	<i>p</i> -
1 CF ₃	d [0.9-1.2], s [1.4-2.3], p [4.0]	d [0.9], s [1.5-2.3]	-
2 C ₂ H ₅	d [0.8-1.3], s [1.5-2.0]	d [0.6-3.1]	-
3 n-C ₄ H ₉	d [1.2-1.5], s [1.9-2.3]	d [0.9-1.2], s [1.5-5.1]	s [1.7-3.1], p [3.6-5.1]
4 n-C ₅ H ₁₁	s [2.6-3.2], p [3.8-5.3]	-	d [2.6-3.8], s [3.8], p [4.5-5.3]
5 n-C ₆ H ₁₃	d [1.7-2.3], ss [2.7-4.4]	d [1.4-2.4], w [3.3-4.1]	d [1.1-3.0], s [4.1-4.7], p [5.4]
6 n-C ₇ H ₁₅	p [2.9-6.2]	-	p [2.9-5.3]
7 n-C ₈ H ₁₇	d [2.3-3.5], w [4.0], p [4.6-5.8]	-	p [1.9-4.1]

^aThe maximum concentrations of the dyes during synthesis are given in the brackets. w: weak gel during synthesis, s: stable gel during synthesis, ss: gel remains stable after synthesis, d: dissolved, p: precipitation.

ANALYTICAL DATA FOR THE AZO-DYES:

1-o:

Yield: 75 % as red crystals.

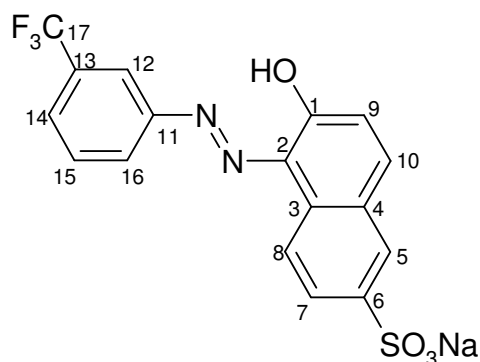
$^1\text{H-NMR}$ (300 MHz, d_6 -DMSO), δ (ppm) = 15,49 (s, 1H, OH), 8,58 (d, 1H, $J=8,60$, 8-H), 8,29 (d, 1H, $J=8,17$, 16-H), 8,12 (d, 1H, $J=9,46$, 10-H), 8,10 (d, 1H, $J=1,72$, 5-H), 7,88 (dd, 1H, $J_1=1,72$, $J_2=8,60$, 7-H), 7,74 (d, 1H, $J=8,17$, 13-H), 7,52-7,59 (m, 1H, 15-H), 7,34-7,44 (m, 1H, 14-H), 7,00 (d, 1H, $J=9,46$, 9-H).

$^{13}\text{C-NMR}$ (75,4 MHz, d_6 -DMSO), δ (ppm) = 166,3 (C-1), 146,2 (C-11), 141,1 (C-6), 134,3 (C-12), 133,5 (C-13), 132,4 (C-10), 130,5 (C-14), 128,3 (C-2), 127,5 (C-5), 127,0 (C-15), 126,6 (C-7), 125,8 (C-3), 123,1 (C-4), 121,3 (C-9), 120,7 (C-8), 120,3 (CF₃), 117,4 (C-16).

IR (KBr) $\tilde{\nu}$ (cm^{-1}) = 3420, 2356, 2343, 1622, 1593, 1554, 1517, 1501, 1484, 1464, 1424, 1312, 1288, 1265, 1252, 1202, 1123, 1109, 1086, 1046, 1030, 1020, 980, 903, 838, 801, 765, 685, 665, 652, 635, 549, 509.

Elemental. Calcd. for $\text{C}_{17}\text{H}_{10}\text{F}_3\text{N}_2\text{NaO}_4\text{S}$: C: 48,81 %, H: 2,41 %, F: 13,62 %, N: 6,70 %, Na: 5,50 %, S: 7,67 %; Found: C: 48,85 %, H: 2,38 %, N: 6,67 %, S: 7,77 %.

mp 333 °C decomposition.

1-m:

Yield: 55 % as red solid.

$^1\text{H-NMR}$ (300 MHz, d_6 -DMSO), δ (ppm) = 15,50 (s, 1H, OH), 8,45 (d, 1H, $J=8,39$, 8-H), 7,99-8,12 (m, 4H, 5-H, 10-H, 12-H, 16-H), 7,85 (d, 1H, $J=8,39$, 7-H), 7,62-7,74 (m, 2H, 14-H, 15-H), 6,85 (d, 1H, $J=9,46$, 9-H).

$^{13}\text{C-NMR}$ (75,4 MHz, d_6 -DMSO), δ (ppm) = 171,2 (C-1), 146,1 (C-11), 145,3 (C-6), 141,3 (C-13),

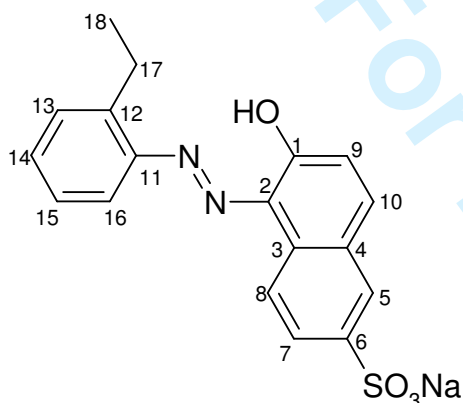
132,6 (C-15), 130,9 (C-10), 130,7 (C-14), 130,2 (C-16), 129,7 (C-2), 127,3 (C-5), 126,9 (C-7), 125,9 (C-3), 125,7 (C-4), 124,7 (C-9), 121,9 (CF₃), 121,3 (C-8), 115,5 (C-12).

IR (KBr) $\tilde{\nu}$ (cm⁻¹) = 3426, 2359, 2338, 1651, 1623, 1557, 1507, 1330, 1255, 1210, 1181, 1125, 1094, 1064, 1042, 985, 899, 843, 795, 734, 691, 667, 658, 643, 601, 514, 484.

Elemental. Calcd. for C₁₇H₁₀F₃N₂NaO₄S: C: 48,81 %, H: 2,41 %, F: 13,62 %, N: 6,70 %, Na: 5,50 %, S: 7,67 %; Found: C: 48,78 %, H: 2,37 %, N: 6,80 %, S: 7,59 %.

mp 358 °C decomposition.

2-o:



Yield: 65 % as red crystals.

¹H-NMR (300 MHz, d₆-DMSO), δ (ppm) = 16,36 (s, 1H, OH), 8,49 (d, 1H, *J*=8,60, 8-H), 8,06 (d, 1H, *J*=1,72, 5-H), 8,02 (d, 1H, *J*=9,03, 10-H), 8,00-8,06 (m, 1H, 16-H), 7,87 (dd, 1H, *J*₁=1,72, *J*₂=8,60, 7-H), 7,23-7,41 (m, 3H, 13-H, 14-H, 15-H), 6,94 (d, 1H, *J*=9,03, 9-H), 2,80 (q, 2H, *J*=7,54, 17-H), 1,25 (t, 3H, *J*=7,54, CH₃).

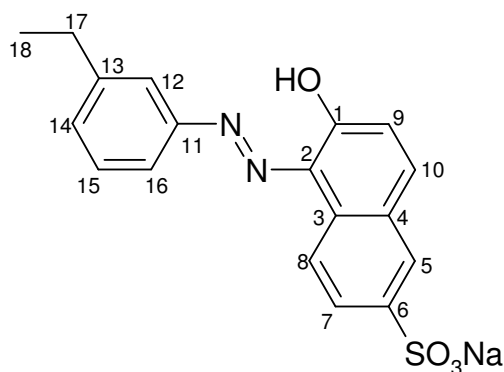
¹³C-NMR (75,4 MHz, d₆-DMSO), δ (ppm) = 169,4 (C-1), 145,5 (C-11), 142,2 (C-6), 140,2 (C-12), 135,4 (C-13), 132,6 (C-10), 129,8 (C-14), 129,6 (C-2), 128,3 (C-5), 127,6 (C-15), 126,9 (C-7), 126,7 (C-3), 125,7 (C-4), 124,2 (C-9), 120,8 (C-8), 115,7 (C-16), 23,9 (C-17), 14,3 (C-18).

IR (KBr) $\tilde{\nu}$ (cm⁻¹) = 3420, 2965, 2363, 2342, 1652, 1635, 1621, 1557, 1540, 1505, 1488, 1472, 1457, 1434, 1299, 1259, 1206, 1161, 1125, 1047, 985, 905, 836, 755, 681, 668, 644, 518, 486, 417.

Elemental. Calcd. for C₁₈H₁₅N₂NaO₄S: C: 57,14 %, H: 4,00 %, N: 7,40 %, S: 8,47 %; Found: C: 56,97 %, H: 4,21 %, N: 7,23 %, S: 8,39 %.

mp 318 °C decomposition.

2-m:



Yield: 70 % as bright red solid.

$^1\text{H-NMR}$ (300 MHz, d_6 -DMSO), δ (ppm) = 15,83 (s, 1H, OH), 8,52 (d, 1H, $J=8,17$, 8-H), 8,05 (d, 1H, $J=1,72$, 5-H), 8,02 (d, 1H, $J=9,46$, 10-H), 7,85 (dd, 1H, $J_1=1,72$, $J_2=8,60$, 7-H), 7,67-7,69 (m, 2H, 16-H, 14-H), 7,41-7,47 (m, 1H, 15-H), 7,20-7,24 (m, 1H, 12-H), 6,95 (d, 1H, $J=9,46$, 9-H), 2,70 (q, 2H, $J=7,59$, 17-H), 1,23 (t, 3H, $J=7,59$, CH_3).

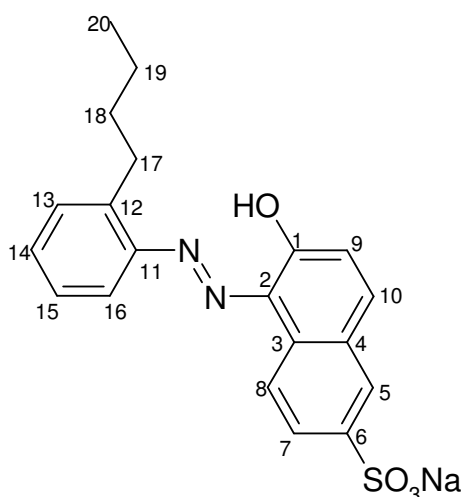
$^{13}\text{C-NMR}$ (75,4 MHz, d_6 -DMSO), δ (ppm) = 168,2 (C-1), 145,7 (C-11), 145,5 (C-6), 145,3 (C-13), 139,9 (C-15), 132,6 (C-10), 129,8 (C-2), 129,1 (C-14), 128,0 (C-5), 127,0 (C-7), 126,6 (C-3), 125,6 (C-4), 124,1 (C-9), 120,9 (C-8), 118,6 (C-12), 116,5 (C-16), 28,0 (C-17), 15,5 (C-18).

IR (KBr) $\tilde{\nu}$ (cm^{-1}) = 3426, 2965, 2932, 2359, 2341, 1683, 1652, 1623, 1558, 1538, 1504, 1471, 1455, 1385, 1256, 1209, 1125, 1092, 1050, 1038, 981, 901, 841, 721, 686, 668, 649, 517, 484, 419.

Elemental. Calcd. for $\text{C}_{18}\text{H}_{15}\text{N}_2\text{O}_4\text{SNa}$: C: 57,14 %, H: 4,00 %, N: 7,40 %, S: 8,47 %; Found: C: 57,88 %, H: 4,15 %, N: 7,68 %, S: 8,17 %.

mp 335 °C decomposition.

3-o:



Yield: 73 % as red crystals.

$^1\text{H-NMR}$ (300 MHz, d_6 -DMSO), δ (ppm) = 16,31 (s, 1H, OH), 8,53 (d, 1H, $J=8,55$, 8-H), 8,06 (d, 1H, $J=1,78$, 5-H), 8,02 (d, 1H, $J=9,39$, 10-H), 8,03-8,15 (m, 1H, 16-H), 7,86 (dd, 1H, $J_1=1,73$, $J_2=8,55$, 7-H), 7,26-7,48 (m, 3H, 13-H, 14-H, 15-H), 6,97 (d, 1H, $J=9,39$, 9-H), 2,83 (t, 2H, $J=7,57$, 17-H), 1,56-1,66 (m, 2H, 18-H), 1,34-1,47 (m, 2H, 19-H), 0,92 (t, 3H, $J=7,30$, CH_3).

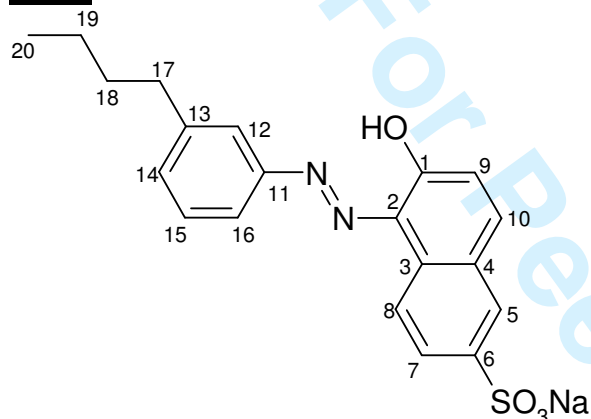
¹³C-NMR (75,4 MHz, d6-DMSO), δ (ppm) = 169,0 (C-1), 145,6 (C-11), 142,5 (C-6), 140,1 (C-12), 134,4 (C-13), 132,6 (C-10), 130,5 (C-14), 129,8 (C-2), 128,2 (C-5), 127,6 (C-15), 126,9 (C-7), 126,7 (C-3), 125,7 (C-4), 124,1 (C-9), 120,8 (C-8), 115,8 (C-16), 32,1 (C-17), 30,7 (C-18), 22,1 (C-19), 13,7 (C-20).

IR (KBr) $\tilde{\nu}$ (cm⁻¹) = 3416, 2955, 2930, 2870, 2359, 2341, 1622, 1556, 1497, 1463, 1385, 1301, 1258, 1206, 1164, 1148, 1126, 1111, 1091, 1046, 985, 904, 837, 804, 761, 694, 680, 641, 603, 518, 486.

Elemental. Calcd. for C₂₀H₁₉N₂NaO₄S: C: 59,10 %, H: 4,71 %, N: 6,89 %, S: 7,89 %; Found: C: 58,93 %, H: 5,03 %, N: 6,72 %, S: 7,87 %.

mp 283 °C decomposition.

3-m:



Yield: 48 % as bright red solid.

¹H-NMR (300 MHz, d6-DMSO), δ (ppm) = 15,83 (s, 1H, OH), 8,52 (d, 1H, $J=8,60$, 8-H), 8,05 (d, 1H, $J=1,72$, 5-H), 8,03 (d, 1H, $J=9,46$, 10-H), 7,84 (dd, 1H, $J_1=1,72$, $J_2=8,60$, 7-H), 7,68-7,70 (m, 2H, 16-H, 14-H), 7,44 (dd, 1H, $J_1=7,74$, $J_2=8,17$, 15-H), 7,20-7,22 (m, 1H, 12-H), 6,95 (d, 1H, $J=9,46$, 9-H), 2,67 (t, 2H, $J=7,60$, 17-H), 1,61 (q, 2H, $J=8,6$, 18-H), 1,30-1,45 (m, 2H, 19-H), 0,91 (t, 3H, $J=7,31$, CH₃).

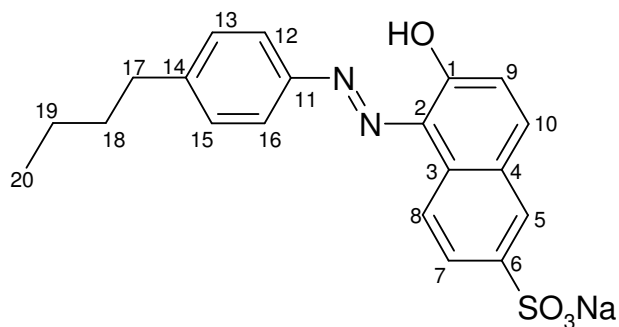
¹³C-NMR (75,4 MHz, d6-DMSO), δ (ppm) = 168,1 (C-1), 145,6 (C-11), 145,3 (C-6), 144,3 (C-13), 139,9 (C-15), 132,6 (C-10), 129,7 (C-2), 129,1 (C-14), 128,4 (C-5), 127,0 (C-7), 126,6 (C-3), 125,6 (C-4), 124,0 (C-9), 120,9 (C-8), 119,2 (C-12), 116,4 (C-16), 34,6 (C-17), 32,9 (C-18), 21,8 (C-19), 13,8 (C-20).

IR (KBr) $\tilde{\nu}$ (cm⁻¹) = 3423, 2955, 2927, 2858, 2358, 2341, 2330, 1652, 1615, 1558, 1505, 1488, 1473, 1457, 1378, 1284, 1255, 1214, 1187, 1125, 1094, 1043, 988, 900, 846, 781, 728, 683, 668, 643, 599, 521, 486, 419.

Elemental. Calcd. for C₂₀H₁₉N₂NaO₄S: C: 59,10 %, H: 4,71 %, N: 6,89 %, S: 7,89 %; Found: C: 59,88 %, H: 4,44 %, N: 6,52 %, S: 8,01 %.

mp 325 °C decomposition.

3-p:



Yield: 88 % as bright red solid.

$^1\text{H-NMR}$ (300 MHz, d_6 -DMSO), δ (ppm) = 15,62 (s, 1H, OH), 8,56 (d, 1H, $J=8,60$, 8-H), 8,10 (d, 1H, $J=1,72$, 5-H), 8,03 (d, 1H, $J=9,46$, 10-H), 7,88 (dd, 1H, $J_1=1,72$, $J_2=8,60$, 7-H), 7,79 (d, 2H, $J=8,60$, 12-H, 16-H), 7,33 (d, 2H, $J=8,60$, 13-H, 15-H), 7,01 (d, 1H, $J=9,46$, 9-H), 2,59 (t, 2H, $J=7,42$, 17-H), 1,54 (q, 2H, $J=7,42$, 18-H), 1,22-1,34 (m, 2H, 19-H), 0,86 (t, 3H, $J=7,31$ CH₃).

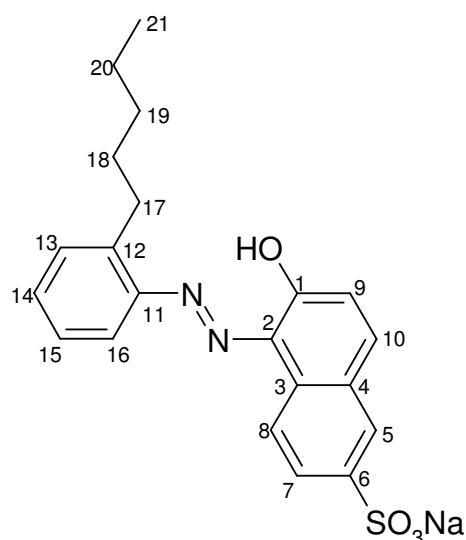
$^{13}\text{C-NMR}$ (75,4 MHz, d_6 -DMSO), δ (ppm) = 164,6 (C-1), 145,1 (C-11), 144,3 (C-6), 143,9 (C-14), 138,8 (C-13, C-15), 132,6 (C-10), 129,6 (C-2), 128,9 (C-5), 127,0 (C-7), 126,5 (C-3), 125,5 (C-4), 123,2 (C-9), 120,8 (C-8), 119,8 (C-12, C-16), 34,6 (C-17), 32,9 (C-18), 21,7 (C-19), 13,7 (C-20).

IR (KBr) $\tilde{\nu}$ (cm⁻¹) = 3419, 2954, 2927, 1622, 1556, 1506, 1377, 1263, 1199, 1126, 1047, 985, 900, 833, 812, 779, 715, 686, 644, 606, 502, 484, 419.

Elemental. Calcd. for C₂₀H₁₉N₂NaO₄S: C: 59,10 %, H: 4,71 %, N: 6,89 %, S: 7,89 %; Found: C: 60,10 %, H: 4,87 %, N: 6,85 %, S: 7,84 %.

mp 334 °C decomposition.

4-o:

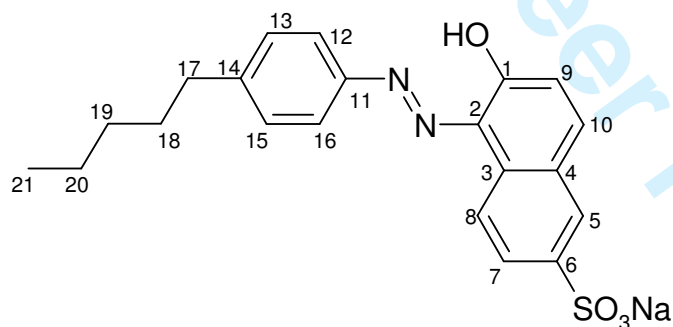


Yield: 61 % as red crystals.

$^1\text{H-NMR}$ (300 MHz, d_6 -DMSO), δ (ppm) = 16,30 (s, 1H, OH), 8,52 (d, 1H, $J=8,60$, 8-H), 8,06 (d, 1H, $J=1,72$, 5-H), 8,03 (d, 1H, $J=9,46$, 10-H), 8,00-8,10 (m, 1H, 16-H), 7,85 (dd, 1H, $J_1=1,72$, $J_2=8,60$, 7-H), 7,25-7,42 (m, 3H, 13-H, 14-H, 15-H), 6,96 (d, 1H, $J=9,46$, 9-H),

1
2
3
4
5
6
7
8
9
10
11
12
13
14
15
16
17
18
19
20
21
22

	2,79 (t, 2H, $J=7,31$, 17-H), 1,55-1,68 (m, 2H, 18-H), 1,22-1,42 (m, 4H, 19-H, 20-H), 0,83 (t, 3H, $J=7,24$, CH ₃).
¹³ C-NMR	(75,4 MHz, d ₆ -DMSO), δ (ppm) = 168,9 (C-1), 145,6 (C-11), 142,5 (C-6), 140,1 (C-12), 134,4 (C-13), 132,6 (C-10), 130,5 (C-14), 129,8 (C-2), 128,2 (C-5), 127,6 (C-15), 126,9 (C-7), 126,7 (C-3), 125,7 (C-4), 124,1 (C-9), 120,8 (C-8), 115,8 (C-16), 31,2 (C-17), 30,9 (C-18), 29,6 (C-19), 21,8 (C-20), 13,9 (C-21).
IR (KBr)	$\tilde{\nu}$ (cm ⁻¹) = 3418, 2929, 1621, 1556, 1496, 1384, 1230, 1257, 1206, 1126, 1045, 986, 904, 838, 758, 681, 643, 488.
Elemental Anal.	Calcd. for C ₂₁ H ₂₁ N ₂ NaO ₄ S: C: 59,99 %, H: 5,03 %, N: 6,66 %, S: 5,47 %; Found: C: 60,21 %, H: 4,99 %, N: 6,65 %, S: 5,54 %.
mp	274 °C decomposition.

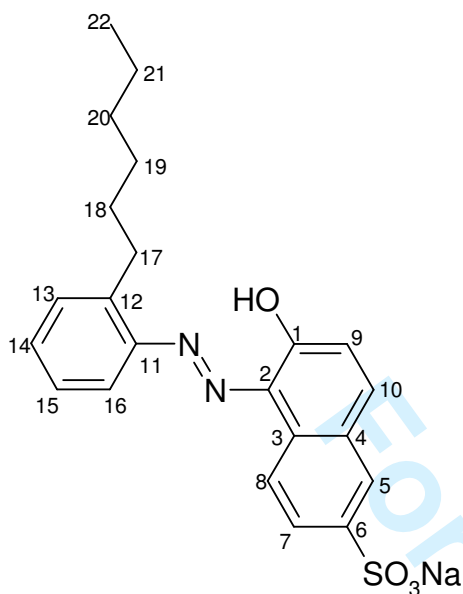
4-p:

36 Yield: 67 % as red crystals.

37
38
39
40
41
42
43
44
45
46
47
48
49
50
51
52
53
54
55
56
57
58
59
60

¹ H-NMR	(300 MHz, d ₆ -DMSO), δ (ppm) = 15,62 (s, 1H, OH), 8,56 (d, 1H, $J=8,60$, 8-H), 8,10 (d, 1H, $J=1,72$, 5-H), 8,02 (d, 1H, $J=9,46$, 10-H), 7,88 (dd, 1H, $J_1=1,72$, $J_2=8,60$, 7-H), 7,78 (d, 2H, $J=8,38$, 12-H, 16-H), 7,31 (d, 2H, $J=8,38$, 13-H, 15-H), 7,01 (d, 1H, $J=9,46$, 9-H), 2,57 (t, 2H, $J=7,74$ 17-H), 1,54 (q, 2H, $J=7,74$, 18-H), 1,19-1,30 (m, 4H, 19-H, 20-H), 0,81 (t, 3H, $J=7,31$ CH ₃).
¹³ C-NMR	(75,4 MHz, d ₆ -DMSO), δ (ppm) = 164,6 (C-1), 145,0 (C-11), 144,3 (C-6), 143,9 (C-14), 138,8 (C-13, C-15), 132,6 (C-10), 129,6 (C-2), 128,9 (C-5), 127,0 (C-7), 126,4 (C-3), 125,5 (C-4), 123,2 (C-9), 120,8 (C-8), 119,8 (C-12, C-16), 34,8 (C-17), 30,8 (C-18), 30,4 (C-19), 21,9 (C-20), 13,9 (C-21).
IR (KBr)	$\tilde{\nu}$ (cm ⁻¹) = 3427, 2955, 2967, 2855, 2360, 2341, 2331, 1623, 1557, 1538, 1507, 1495, 1487, 1472, 1455, 1259, 1199, 1181, 1127, 1048, 1040, 986, 902, 833, 807, 682, 668, 645, 604, 518, 502, 486, 457.
Elemental Anal.	Calcd. for C ₂₁ H ₂₁ N ₂ NaO ₄ S: C: 59,99 %, H: 5,03 %, N: 6,66 %, S: 5,47 %; Found: C: 59,95 %, H: 5,37 %, N: 6,71 %, S: 5,43 %.
mp	307 °C decomposition.

5-o:

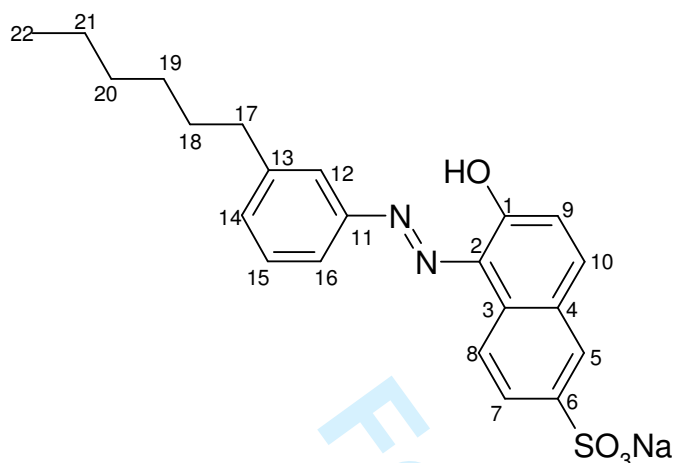


Yield: 9,88 g, 65 % as red crystals.

- ¹H-NMR (300 MHz, d₆-DMSO), δ (ppm) = 15,89 (s, 1H, OH), 8,52 (d, 1H, $J=8,56$, 8-H), 8,09 (d, 1H, $J=1,64$, 5-H), 8,02 (d, 1H, $J=9,39$, 10-H), 7,88 (dd, 1H, $J_1=1,64$, $J_2=8,56$, 7-H), 7,61-7,66 (m, 2H, 15-H, 16-H), 7,36-7,43 (m, 1H, 14-H), 7,15-7,17 (m, 1H, 13-H), 6,95 (d, 1H, $J=9,39$, 9-H), 2,61 (t, 2H, $J=7,61$, 17-H), 1,52-1,64 (m, 2H, 18-H), 1,20-1,38 (m, 6H, 19-H, 20-H, 21-H), 0,81 (t, 3H, $J=7,31$, CH₃).
- ¹³C-NMR (75,4 MHz, d₆-DMSO), δ (ppm) = 168,02 (C-1), 145,27 (C-11), 145,13 (C-6), 144,20 (C-10), 139,73 (C-2), 132,63 (C-12), 129,54 (C-14), 129,04 (C-5), 128,36 (C-7), 126,90 (C-3), 126,48 (C-4), 125,61 (C-13), 123,96 (C-15), 120,80 (C-9), 118,98 (C-16), 116,33 (C-8), 34,88 (C-20), 31,02 (C-18), 30,66 (C-17), 28,25 (C-19), 22,00 (C-21), 13,84 (C-22).
- IR (KBr) $\tilde{\nu}$ (cm⁻¹) = 3426, 2946, 2920, 2858, 2361, 2326, 1611, 1506, 1384, 1218, 1157, 21139, 1035, 991, 843, 773, 729, 694, 659, 651, 598, 520, 485.
- Elemental. Calcd. for C₂₂H₂₃N₂NaO₄S: C: 60,82 %, H: 5,34 %, N: 6,45 %, S: 7,38 %; Found: C: 60,53 %, H: 5,24 %, N: 6,38 %, S: 7,37 %.
- mp 290 °C decomposition.

5-m:

Yield: 6,38 g, 42 % as bright red solid.



¹H-NMR (300 MHz, d₆-DMSO), δ (ppm) = 16,27 (s, 1H, OH), 8,50 (d, 1H, $J=8,60$, 8-H), 8,07 (d, 1H, $J=1,72$, 5-H), 8,00 (d, 1H, $J=9,46$, 10-H), 7,98 (d, 1H, $J=5,0$, 16-H), 7,87 (dd, 1H, $J_1=1,72$, $J_2=8,60$, 7-H), 7,21-7,37 (m, 3H, 12-H, 14-H, 15-H), 6,93 (d, 1H, $J=9,46$, 9-H), 2,73 (t, 2H, $J=7,60$, 17-H), 1,55 (q, 2H, $J=7,7$, 18-H), , 1,32 (q, 2H, $J=7,3$, 19-H), 1,10-1,30 (m, 4H, 20-H, 21-H), 0,78 (t, 3H, $J=7,31$, CH₃).

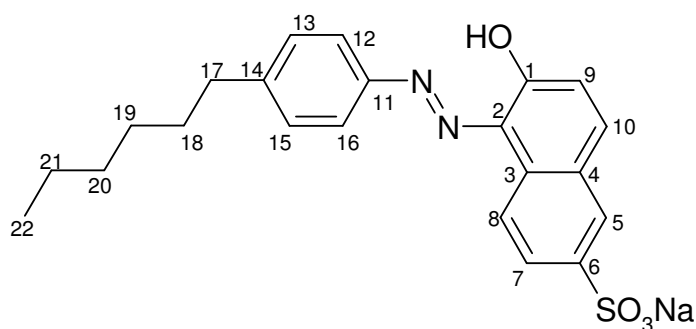
¹³C-NMR (75,4 MHz, d₆-DMSO), δ (ppm) = 168,1 (C-1), 145,5 (C-11), 145,2 (C-6), 144,3 (C-13), 139,9 (C-15), 132,6 (C-10), 129,6 (C-2), 129,1 (C-14), 128,5 (C-5), 127,0 (C-7), 126,6 (C-3), 125,6 (C-4), 124,0 (C-9), 120,9 (C-8), 119,1 (C-12), 116,4 (C-16), 34,9 (C-17), 31,1 (C-18), 30,7 (C-19), 28,3 (C-20), 22,1 (C-21), 13,9 (C-22).

IR (KBr) $\tilde{\nu}$ (cm⁻¹) = 3423, 2956, 2925, 2853, 1624, 1560, 1507, 1379, 1264, 1200, 1179, 1127, 1048, 988, 902, 835, 783, 728, 685, 653, 483.

Elemental. Calcd. for C₂₂H₂₃N₂NaO₄S: C: 60,82 %, H: 5,34 %, N: 6,45 %, S: 7,38 %; Found: C: 60,72 %, H: 5,61 %, N: 6,20 %, S: 7,11 %.

mp 294 °C decomposition.

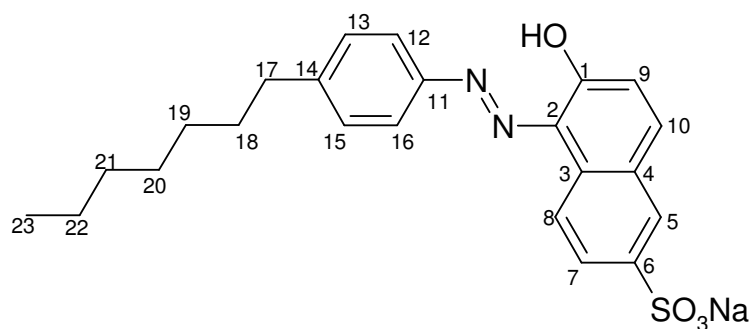
5-p:



Yield: 75 % as red crystals.

¹H-NMR (300 MHz, d₆-DMSO), δ (ppm) = 15,62 (s, 1H, OH), 8,56 (d, 1H, $J=8,60$, 8-H), 8,09 (d, 1H, $J=1,29$, 5-H), 8,03 (d, 1H, $J=9,46$, 10-H), 7,86 (dd, 1H, $J_1=1,29$, $J_2=8,60$, 7-H), 7,82 (d, 2H, $J=8,17$, 12-H, 16-H), 7,34 (d, 2H, $J=8,17$, 13-H, 15-H), 7,01 (d, 1H, $J=9,46$, 9-H), 2,59 (t, 2H, $J=7,52$, 17-H), 1,55 (q, 2H, $J=7,52$, 18-H), 1,17-1,30 (m, 6H, 19-H, 20-H, 21-H), 0,81 (t, 3H, $J=7,30$ CH₃).

¹³C-NMR (75,4 MHz, d₆-DMSO), δ (ppm) = 164,6 (C-1), 145,1 (C-11), 144,3 (C-6), 143,9 (C-14), 138,8 (C-13, C-15), 132,6 (C-10), 129,6 (C-2), 128,9 (C-5), 127,0 (C-7), 126,5 (C-3), 125,5 (C-4), 123,2 (C-9), 120,8 (C-8), 119,8 (C12, C-16), 34,9 (C-17), 31,1 (C-18), 30,8 (C-19), 28,3 (C-20), 22,1 (C-21), 13,9 (C-22).



Yield: 61 % as red crystals.

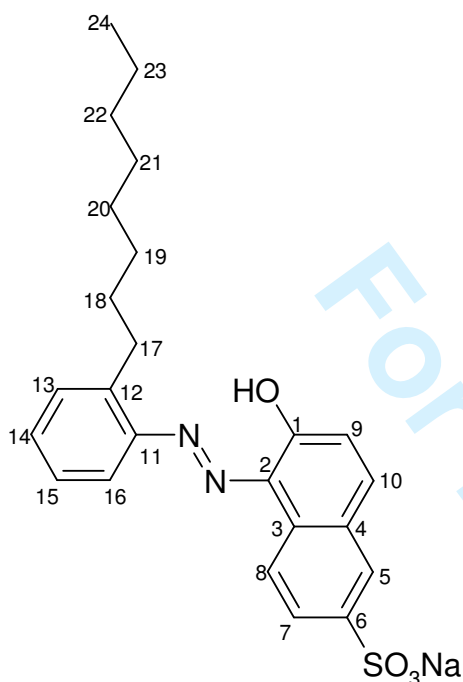
¹H-NMR (300 MHz, d₆-DMSO), δ (ppm) = 15,69 (s, 1H, OH), 8,56 (d, 1H, $J=8,60$, 8-H), 8,08 (d, 1H, $J=1,29$, 5-H), 8,03 (d, 1H, $J=9,46$, 10-H), 7,85 (dd, 1H, $J_1=1,29$, $J_2=8,60$, 7-H), 7,82 (d, 2H, $J=8,60$, 12-H, 16-H), 7,35 (d, 2H, $J=8,60$, 13-H, 15-H), 7,02 (d, 1H, $J=9,46$, 9-H), 2,61 (t, 2H, $J=7,52$, 17-H), 1,58 (q, 2H, $J=7,52$, 18-H), 1,15-1,32 (m, 8H, 19-H, 20-H, 21-H, 22-H), 0,83 (t, 3H, $J=7,31$ CH₃).

¹³C-NMR (75,4 MHz, d₆-DMSO), δ (ppm) = 164,6 (C-1), 145,3 (C-11), 144,4 (C-6), 143,9 (C-14), 138,9 (C-13, C-15), 132,5 (C-10), 129,6 (C-2), 129,6 (C-5), 127,0 (C-7), 126,5 (C-3), 125,5 (C-4), 123,1 (C-9), 120,8 (C-8), 119,8 (C-12, C-16), 34,9 (C-17), 31,3 (C-18), 30,8 (C-19), 28,6 (C-20), 28,5 (C-21), 22,1 (C-22), 13,9 (C-23).

IR (KBr) $\tilde{\nu}$ (cm⁻¹) = 3406, 2955, 2922, 2851, 1620, 1551, 1508, 1466, 1387, 1261, 1205, 1146, 1128, 1092, 1049, 986, 903, 835, 808, 721, 683, 642, 602, 561, 503, 484, 424.

Elemental. Calcd. for C₂₃H₂₅N₂NaO₄S: C: 61,59 %, H: 5,62 %, N: 6,25 %, S: 7,15 %; Found: C: 61,38 %, H: 5,01 %, N: 6,27 %, S: 7,88 %.

mp 305 °C decomposition.

7-o:

Yield: 42 % as red crystals.

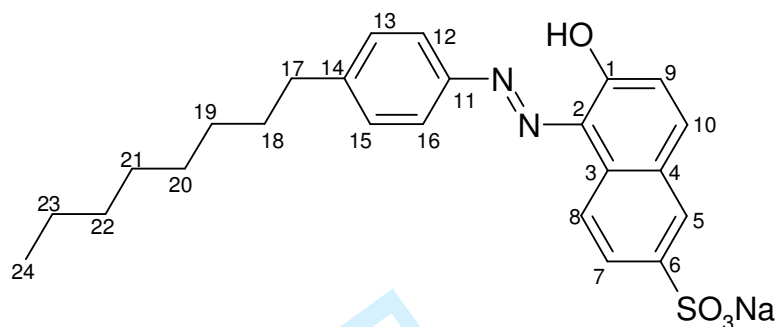
$^1\text{H-NMR}$ (300 MHz, d_6 -DMSO), δ (ppm) = 15,85 (s, 1H, OH), 8,51 (d, 1H, $J=8,60$, 8-H), 8,06 (d, 1H, $J=1,72$, 5-H), 8,03 (d, 1H, $J=9,46$, 10-H), 7,85 (dd, 1H, $J_1=1,72$, $J_2=8,60$, 7-H), 7,63-7,71 (m, 2H, 15-H, 16-H), 7,37-7,46 (m, 1H, 14-H), 7,15-7,22 (m, 1H, 13-H), 6,95 (d, 1H, $J=9,46$, 9-H), 2,63 (t, 2H, $J=8,17$, 17-H), 1,56-1,61 (m, 2H, 18-H), 1,05-1,35 (m, 10H, 19-H, 20-H, 21-H, 22-H), 0,80 (t, 3H, $J=7,30$, CH_3).

$^{13}\text{C-NMR}$ (75,4 MHz, d_6 -DMSO), δ (ppm) = 168,1 (C-1), 145,5 (C-11), 145,2 (C-6), 144,3 (C-12), 139,9 (C-13), 132,6 (C-10), 129,6 (C-14), 129,1 (C-2), 128,4 (C-5), 127,0 (C-15), 126,6 (C-7), 125,6 (C-3), 124,0 (C-4), 120,8 (C-9), 119,1 (C-8), 116,4 (C-16), 35,0 (C-17), 31,3 (C-18, C-19), 30,8 (C-20), 28,8 (C-21), 28,7 (C-22), 22,1 (C-23), 13,9 (C-24).

IR (KBr) $\tilde{\nu}$ (cm^{-1}) = 3444, 2958, 2923, 2852, 2363, 2338, 1653, 1620, 1557, 1504, 1490, 1470, 1384, 1253, 1210, 1128, 1092, 1045, 987, 902, 833, 779, 727, 686, 667, 644, 520, 482, 417.

Elemental. Calcd. for $\text{C}_{24}\text{H}_{27}\text{N}_2\text{O}_4\text{SNa}$: C: 62,32 %, H: 5,88 %, N: 6,06 %, S: 6,93 %; Found: C: 62,55 %, H: 5,71 %, N: 6,02 %, S: 6,51 %.

mp 273 °C decomposition.

7-p:

Yield: 40 % as red crystals.

$^1\text{H-NMR}$ (300 MHz, d_6 -DMSO), δ (ppm) = 15,62 (s, 1H, OH), 8,56 (d, 1H, $J=8,60$, 8-H), 8,07 (d, 1H, $J=1,29$, 5-H), 7,99 (d, 1H, $J=9,46$, 10-H), 7,84 (dd, 1H, $J_1=1,29$, $J_2=8,60$, 7-H), 7,84 (d, 2H, $J=8,60$, 12-H, 16-H), 7,33 (d, 2H, $J=8,60$, 13-H, 15-H), 7,00 (d, 1H, $J=9,46$, 9-H), 2,55 (t, 2H, $J=7,52$, 17-H), 1,58 (q, 2H, $J=7,52$, 18-H), 1,19-1,28 (m, 10H, 19-H, 20-H, 21-H, 22-H, 23-H), 0,81 (t, 3H, $J=7,31$ CH₃).

$^{13}\text{C-NMR}$ (75,4 MHz, d_6 -DMSO), δ (ppm) = 164,6 (C-1), 144,9 (C-11), 144,7 (C-6), 143,7 (C-14), 138,5 (C-13, C-15), 132,8 (C-10), 129,6 (C-2), 129,0 (C-5), 126,8 (C-7), 126,3 (C-3), 125,4 (C-4), 123,5 (C-9), 120,7 (C-8), 119,9 (C-12, C-16), 39,5 (C-17), 34,9 (C-18), 31,3 (C-19), 30,8 (C-20), 28,8 (C-21), 28,6 (C-22), 22,1 (C-23), 13,9 (C-24).

IR (KBr) $\tilde{\nu}$ (cm⁻¹) = 3419, 2956, 2922, 2851, 1621, 1552, 1507, 1379, 1263, 1199, 1128, 1048, 986, 901, 833, 810, 731, 688, 646, 502.

Elemental. Calcd. for C₂₄H₂₇N₂O₄SNa: C: 62,32 %, H: 5,88 %, N: 6,06 %, S: 6,93 %; Found: C: 61,85 %, H: 6,08 %, N: 5,81 %, S: 7,27 %.

mp 322 °C decomposition.